

Intelligent design of cooling systems for aluminum alloy die-casting dies: A framework integrating topology optimization and particle swarm optimization

Le-chuan Li¹, *Ya-jun Yin¹, Xu Shen¹, Wen Li¹, Xiao-yuan Ji¹, Chao-jian Liang², Wei Wei², and Jian-xin Zhou¹

1. State Key Laboratory of Materials Processing and Die & Mould Technology, Huazhong University of Science and Technology, Wuhan 430074, China

2. Xiangyang Millison Science & Technology Co., Xiangyang 441000, Hubei, China

Copyright © 2026 Foundry Journal Agency

Abstract: With the growing demand for lightweight and high-performance components in automotive and aerospace industries, aluminum alloy die-castings are evolving toward larger dimensions and thinner walls, posing significant challenges to thermal management during solidification. Traditional cooling channel designs often fail to ensure uniform temperature distribution, leading to defects such as shrinkage porosity and deformation. This study proposes an automated design framework integrating the moving morphable components (MMC) topology optimization method with particle swarm optimization (PSO) to generate efficient and manufacturable cooling channel layouts for A380 aluminum alloys. Firstly, a systematic initialization strategy was developed with component dimensions of 4–10 mm in width and 15–40 mm in length, along with discrete orientation angles. The optimization process effectively guided components toward high-temperature regions identified through numerical simulation, followed by post-processing operations including temperature-based sorting, overlap removal, and component interconnection. The final design with 20 retained components was selected. Then, castings with a conventional cooling system and without any cooling system were employed as benchmark cases for comparison with the current optimized design. Compared with the conventional and no-cooling cases, the current cooling system exhibits a consistently lower temperature standard deviation after 30 s, maintains superior thermal uniformity throughout solidification, and achieves this improvement without comprising the average temperature.

Keywords: topology optimization; cooling channel design; die casting; moving morphable components; aluminum alloy

CLC numbers: TG146.21

Document code: A

Article ID: 1672-6421(2026)03-385-11

1 Introduction

With the continuous advancement of lightweight and complex structural components in the fields of new energy vehicles, aerospace, and high-end equipment manufacturing, the casting and forming of lightweight metallic materials are encountering increasingly stringent technical challenges. Among these materials, aluminum alloys, characterized by

low density, high specific strength, and excellent corrosion resistance, have been extensively employed in aerospace applications (e.g., aircraft fuselages, engine components, satellite structures) as well as in automotive manufacturing (e.g., body-in-white, engine, and chassis systems)^[1-2]. Driven by the growing demand for lightweight design and enhanced performance, aluminum alloy castings are evolving toward larger dimensions, higher structural complexity, and thinner wall thicknesses. For instance, integrated die-cast aluminum components, which feature large size and intricate geometries, require highly precise control of material microstructure and impose stringent demands on casting processes^[3-4]. Consequently, the fabrication of such large and complex thin-walled

*Ya-jun Yin

Male, born in 1985, Associate Professor, and doctoral supervisor. Research interest: Numerical simulation of casting.

E-mail: yinyajun436@hust.edu.cn

Received: 2025-11-07; Revised: 2026-01-04; Accepted: 2026-01-26

aluminum alloy components necessitates advanced die cooling system designs and meticulous optimization of process parameters to ensure structural integrity and casting quality^[5-6].

During the aluminum alloy die casting process, thermal imbalance frequently occurs during the filling and solidification stages. The cooling system, consisting of channels embedded within the mold, circulates a cooling medium to reduce the temperature of specific regions, thereby controlling the temperature field during the solidification process of the casting. A properly designed cooling system ensures uniform contraction of the casting during solidification, effectively preventing defects such as shrinkage cavities, hot cracks, and cold shuts. Therefore, the design of the cooling system has a direct and significant impact on both the quality and productivity of castings. A well-optimized cooling system design can accelerate the solidification rate of the casting, thus shortening the production cycle. Furthermore, by optimizing the layout and flow path of the cooling channels, the cooling efficiency can be enhanced, the cooling time reduced, and the overall production efficiency improved.

Numerous studies have been conducted worldwide on the simulation and automated design of die cooling channels. Federica et al.^[7] compared two alternative cooling system configurations for die inserts used in the die casting of light alloy components. The results demonstrate that the cooling channels play a significant role in reducing mechanical stresses and defects in the castings, as well as in shortening the manufacturing cycle. Chavan et al.^[8] designed and optimized the placement of cooling channels in a cold-chamber high-pressure die casting machine. The results show that the position of the cooling channels has a significant influence on the stress generated within the die. Pelaccia et al.^[9] investigated the efficiency of conformal cooling channel inserts applied to extrusion dies. The results showed a good experimental numerical matching had been achieved with peak errors of 7.5% and 14% in terms of temperature and extrusion load, respectively. Yavuz et al.^[10] numerically evaluated the performance of a cooling system for aluminum low-pressure casting, noting that the flow rate of the cooling system is affected by the inlet count, the pressure of the cooling channel, and the ratio between the inlet and outlet areas. Kurtulus et al.^[11] experimentally assessed the cooling and heating performance of a gravity die casting die equipped with conformal cooling channels. They observed that a more homogeneous die surface temperature distribution was achieved in the conformal cooling die, as well as a 28% shorter cycle time. Shu et al.^[12] proposed a conformal cooling design for die-casting die inserts to enhance thermal regulation. Compared with conventional cooling channels, the conformal cooling channels were distributed closer to the die surface to be cooled, providing better cooling performance, with an effective cooling efficiency of 54.83%. Dhisale et al.^[13] optimized cooling channel parameters in the low-pressure die casting process to minimize shrinkage porosity in aluminum alloy wheels. The improvement of the cooling

process significantly reduced the shrinkage porosity rate of the castings. Arunkumar et al.^[14] examined the flow and heat transfer characteristics of cooling channels in high-pressure die casting molds. By optimizing parameters such as flow rate and nozzle diameter, the maximum heat dissipation rate of the chip was achieved.

The design of a die cooling system fundamentally concerns the arrangement and optimization of internal flow channel structures. Owing to its ability to handle complex geometric layouts and multi-physics constraints, topology optimization provides an effective approach for solving this class of design problems. The moving morphable components (MMC) method is one of the fundamental approaches in topology optimization, originally proposed by Guo et al.^[15-19]. Compared with the conventional variable density method, MMC features fewer design variables and significantly reduced mesh dependency. Moreover, it is capable of explicitly representing topology evolution during the optimization process^[20]. Takaloozadeh et al.^[21] developed a new topology optimization approach based on the MMC framework incorporating topological derivatives, which efficiently computes shape and position sensitivities without discrete finite element analysis. Wang et al.^[22] presented an MMC-based topology optimization method that employs a virtual component skeleton (VCS) and effective connection status (ECS) control scheme, enabling direct and accurate regulation of the minimum length scale irrespective of component geometry. Sun et al.^[23] developed an explicit topology optimization method based on the MMC framework for the design of fiber-reinforced composite materials, which enables simultaneous optimization of structural layout and fiber orientation while ensuring component independence. It can be concluded from the above studies that the MMC method exhibits high flexibility and performs effectively across various physical scenarios.

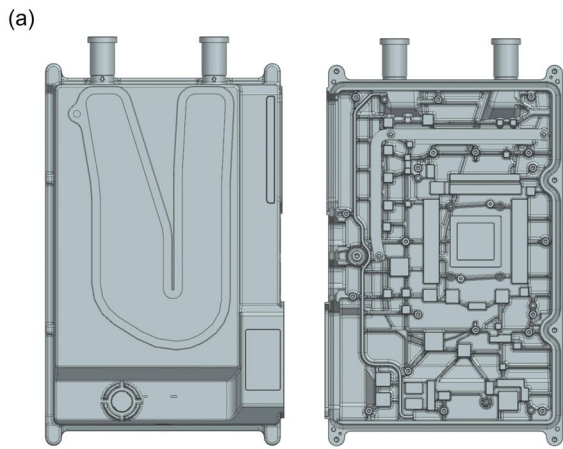
In this study, we developed a model for designing the cooling channels of die casting aluminum alloy bottom shell based on the MMC method.^[1] Firstly, the structural features and forming characteristics of the die casting aluminum alloy bottom shell were analyzed, and the filling and solidification processes were numerically simulated. Secondly, according to the simulation results, the heat transfer behavior during solidification was investigated, and the high-temperature regions within the die casting were identified. Thirdly, based on the obtained overheating regions, an automatic cooling system design model was established using the MMC-based topology optimization approach. Finally, the effectiveness of the proposed model and the rationality of the designed cooling system were verified by comparing the topology optimization results with the overheating regions observed in the die casting process.

2 Method and model

2.1 Analysis of casting structure

The casting investigated in this study was an aluminum alloy bottom shell die casting used in automotive applications. The

three-dimensional geometry of the casting is illustrated in Fig. 1(a). As observed, the overall dimensions of the component are relatively large, particularly along the length and width directions, which results in a longer filling process.



The casting features an extremely thin wall, with the minimum wall thickness being only 2.8 mm. Consequently, insufficient injection velocity or uneven temperature distribution may easily lead to defects such as cold shuts.

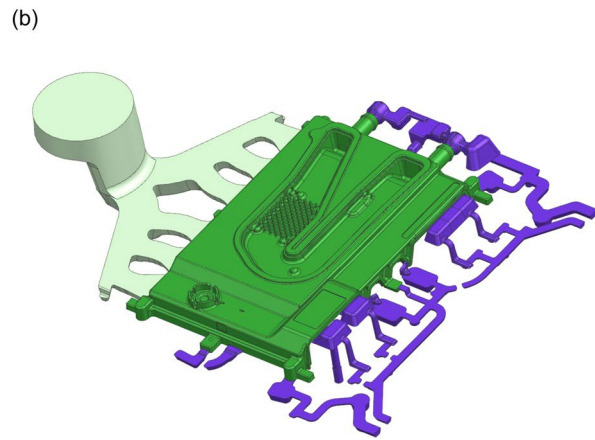


Fig. 1: Aluminum alloy bottom shell die casting (a) and its gating system (b)

Moreover, a considerable number of positioning holes and internal structures are embedded within the shell, imposing stringent requirements on dimensional accuracy during machining. Local overheating during die casting may induce thermal deformation, causing significant dimensional deviations that adversely affect subsequent assembly precision. Considering these structural characteristics, the gating and runner system was designed for the die casting aluminum alloy bottom shell, as shown in Fig. 1(b), to minimize the filling path and promote simultaneous solidification. Overflow grooves were arranged in the last filling regions and thick sections prone to porosity, effectively reducing shrinkage cavities and internal pores to the greatest possible extent.

2.2 Topology description

In the proposed model, the design objective is the cooling channel of the die, which is represented as a continuous and uninterrupted conduit extending from the inlet to the outlet. The layout of the channel can be freely arranged within the allowable design domain. To simplify the design objective, only two-dimensional configurations of the cooling channel are considered in this study. As illustrated in Fig. 2, the design variables corresponding to a single casting are defined, from which the descriptive equation of an individual component can be expressed as:

$$D_i = [X_0, Y_0, L_0, D_0, \theta_0] \quad (1)$$

where D_i is the set of descriptive parameters of a single component, X_0 and Y_0 denote the central position of a single casting within the two-dimensional design domain, L_0 is the length of the individual component, D_0 is the side length of the square cross-section of the casting (assuming a square cross-section), and θ_0 is the angle between the casting's longitudinal direction and horizontal axis. The position of the component above is defined in the global coordinate system. To facilitate optimization, it is necessary

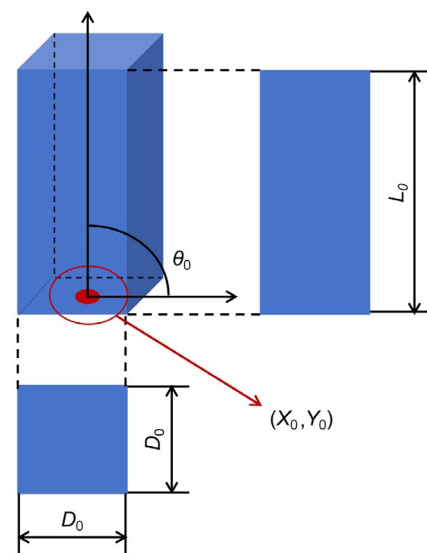


Fig. 2: Topological description of a single component

to transform the component's global coordinates into its local coordinate system, as expressed by the following equations:

$$\begin{cases} X' \\ Y' \end{cases} = \begin{bmatrix} \cos \theta & \sin \theta \\ -\sin \theta & \cos \theta \end{bmatrix} \begin{cases} X - X_0 \\ Y - Y_0 \end{cases} \quad (2)$$

where X' and Y' are the relative coordinates with respect to the component's centroid, while the X and Y are the global absolute coordinates.

Subsequently, a Heaviside function is introduced within the design domain to differentiate the solid material regions from the voids. In order to ensure that the shape function is differentiable everywhere, a typical smooth function was chosen as the Heaviside function. The corresponding shape equation is defined as follows:

$$H_\beta(\phi^s(x; D)) = \frac{1}{2} \left(1 + \frac{2}{\pi} \arctan(\beta \phi^s(x; D)) \right) \quad (3)$$

where β is a parameter used to control the smoothness of

the Heaviside function. When β is large, the Heaviside function approaches a step function. When β is small, the Heaviside function becomes smoother, which is conducive to convergence. $\phi^s(x; D)$ is shape function, x is spatial coordinate point, D is design variables. The detailed definition of the shape function is as follows:

$$\begin{cases} \phi^s(x; D) > 0, & \text{if } x \in \Omega^s, \\ \phi^s(x; D) = 0, & \text{if } x \in \partial\Omega^s, \\ \phi^s(x; D) < 0, & \text{if } x \in D \setminus \Omega^s, \end{cases} \quad (4)$$

where Ω^s is solid domain in the design domain, and $\partial\Omega^s$ is boundary, $D \setminus \Omega^s$ is void domain in the design domain. After establishing the topological description of the components, we can describe the topology of all components and formulate the corresponding optimization problem as follows:

$$\begin{aligned} \min_D C(D) &= \int_{\Omega} H(\phi^s(x; D)) \mathbf{f} \cdot \mathbf{u}(x; D) dV \\ \text{s.t. } \int_{\Omega} H(\phi^s(x; D)) dV &\leq V^*, \mathbf{K}(D)\mathbf{u} = \mathbf{F}, D_{\min} \leq D \leq D_{\max} \end{aligned} \quad (5)$$

where $C(D)$ is compliance. The objective of this equation is to minimize the structural compliance. \mathbf{f} is external load vector, $\mathbf{u}(x; D)$ is displacement field. In the constraint equations, V^* is maximum allowable material volume, $\mathbf{K}(D)$ is structural stiffness matrix, \mathbf{u} is displacement vector. \mathbf{F} is external force vector, D_{\max} and D_{\min} are lower and upper bounds of the design variables. Due to the particularity of the problems in this study, the structural stiffness matrix, displacement vector, and external load vector need to be determined based on simulation and particle swarm optimization.

The MMC method, originally developed for load-bearing mechanical structure design, is extended to the design of cooling channels in die-casting dies. Unlike conventional formulations that focus solely on structural stiffness optimization, the proposed approach incorporates the thermal behavior of the die during the casting process into the topology optimization framework by establishing a physical analogy between temperature fields and mechanical loading conditions. Specifically, the transient or steady-state temperature field obtained from thermal simulations is transformed into an equivalent pseudo-mechanical load field, in which regions with higher temperatures are treated as being subjected to larger virtual loads or assigned higher “thermal weights”.

Based on this analogy, the cooling channel design problem can be reformulated within the MMC framework as an equivalent load-transfer path optimization problem, thereby enabling the optimized channel layout to naturally evolve toward regions of intense heat accumulation. Under this interpretation, the cooling channel functions analogously to an optimal load-bearing structure in classical MMC-based

topology optimization, redistributing the equivalent thermal loads by enhancing heat extraction in critical regions. Accordingly, the movable morphable components are driven to evolve, translate, rotate, and deform along dominant heat-flow paths during the optimization process, while maintaining geometric continuity from the inlet to the outlet.

2.3 Particle swarm optimization

The particle swarm optimization (PSO) algorithm which is based on swarm intelligence^[24, 25], is employed to solve the optimization problem after the topological description of the components has been established. It is inspired by the foraging behavior of birds and the schooling behavior of fish. The algorithm simulates a swarm of particles flying through the solution space and searching for the optimal solution by exchanging information among themselves. PSO has achieved significant success in solving a wide range of optimization problems, particularly those that are high-dimensional, multimodal, nonlinear, and non-convex. The main equation of the PSO method is as follows:

$$\begin{aligned} v_j^{(t+1)} &= \omega v_j^{(t)} + c_1 r_1 (pbest_j - D_j^{(t)}) + c_2 r_2 (gbest - D_j^{(t)}) \\ D_j^{(t+1)} &= D_j^{(t)} + v_j^{(t+1)} \end{aligned} \quad (6)$$

where $v^{(t+1)}$ is velocity of the particle at the next time step, v^t is velocity of the particle at current time step, $pbest_j$ is the historical optimal value of the particle itself, $gbest$ is global optimal value, ω is inertia weight, c_1 and c_2 are learning factors, $D^{(t)}$ is the position of the particle at time t , r_1 and r_2 are random numbers uniformly distributed in the interval $[0, 1]$. The chosen convergence criterion was defined by the maximum number of iterations.

The design model of this study aims to utilize the particle swarm algorithm to conduct a comprehensive exploration of the temperature field on the surface of the casting. During the actual calculation process, the optimization object is presented in the form of components rather than particles. Therefore, the strong exploration ability in a single step reduces the dependence on inertia. Thus, the value of ω should be relatively small. Furthermore, since the global maximum temperature located far from a given component provides negligible insight for its design, the local learning factor should be substantially greater than the global learning factor in the proposed model. Based on the analysis above, the values of the relevant parameters in the particle swarm optimization algorithm are presented in Table 1.

2.4 Assumptions of the model

In order to make the design model more reasonable, certain assumptions and restrictions must be established to clearly define its applicable scope. The main assumptions are as

Table 1: Main parameter settings in the PSO algorithm

| Parameters | ω | c_1 | c_2 | r_1 | r_2 |
|------------|----------|-------|-------|-----------------------------|-----------------------------|
| Value | 0.1 | 0.9 | 0.05 | Random number within [0, 1] | Random number within [0, 1] |

follows:

(1) Since the casting exhibits a large dimension in length and width but a relatively small dimension in height, the design of the cooling flow channels is considered only in the two-dimensional plane.

(2) In this model, finite element stress analysis is not involved. To satisfy the requirements of the topology optimization framework, the temperature field obtained from numerical simulation is employed as the basis for structural response analysis, where the temperature values at different locations of the casting are used as the equivalent external loads.

(3) To simplify the model, the orientation angle of each component is restricted to a finite set of discrete values (e.g., two or four). This discretization effectively covers the design space and greatly enhances computational efficiency.

(4) The present model considers only conformal cooling systems, excluding other types of cooling strategies such as localized or point cooling.

(5) The present model neglects the effects of the cooling medium and coolant flow velocity, focusing solely on the influence of the cooling channel arrangement on the thermal field of the casting.

3 Numerical simulation of the casting process

3.1 Setting of simulation parameters

The A380 aluminum alloy was used for the casting in this study. A380 aluminum alloy exhibits excellent fluidity, allowing the manufacture of thin-walled and intricately shaped components with minimal casting defects. It also has a low tendency toward hot cracking and moderate solidification shrinkage, which contribute to superior die filling and feeding characteristics during the die-casting process. The elemental composition and physical parameters of A380 alloy are shown in Tables 2 and 3, respectively.

Table 2: Elemental composition of A380 alloy

| Element | Si | Cu | Mg | Fe | Mn | Zn | Ni | Sn | Nb | Ni | Al |
|--------------|---------|-----|-----|-----|-----|-----|-----|-----|-----|-----|------|
| Value (wt.%) | 7.5–9.5 | 3–4 | 0.1 | 1.3 | 0.5 | 3.0 | 0.5 | 0.3 | 0.3 | 0.3 | Bal. |

Table 3: Physical parameters of A380 alloy

| Density (g·cm ⁻³) | Specific heat capacity [Cal·(g·°C) ⁻¹] | Thermal conductivity [Cal·(cm·s·°C) ⁻¹] | Viscosity (cm ² ·s ⁻¹) | Latent heat (Cal·g ⁻¹) | Liquidus (°C) | Solidus (°C) | Shrinkage rate of phase transition |
|-------------------------------|--|---|---|------------------------------------|---------------|--------------|------------------------------------|
| 2.750 | 0.240 | 0.350 | 0.004 | 95 | 595 | 530 | 0.010 |

4 Optimization results and discussion

4.1 Initialization of components

Before the optimization process, it is necessary to initialize the size, position, and orientation of the components. Proper

3.2 Simulation of filling and solidification process

The filling process of the A380 aluminum alloy bottom shell casting was numerically simulated, and the coupled results of flow and heat transfer are shown in Fig. 3. As illustrated, significant variations exist in the filling behavior across different regions of the casting. The flow path to the most distant regions is considerably longer, resulting in a pronounced filling time difference. The overall temperature near the runner side remains relatively high, whereas the temperature in regions farther from the runner is markedly lower. Such a temperature gradient may cause thermal imbalance during filling, potentially inducing deformation and other casting defects. Furthermore, as shown in Fig. 3(d), local overheating occurs in several thick sections at the upper part of the casting. Therefore, a dedicated cooling system should be designed to optimize the filling and solidification processes, ensuring uniform temperature distribution and improved casting quality.

By analyzing the filling and solidification simulation results, the temperature field of the bottom shell casting during the die-casting process was obtained, as shown in Fig. 4. The red regions highlighted in Fig. 4 represent the overheated zones identified by the simulation algorithm. As illustrated, these overheated regions are primarily concentrated at the junctions of the internal support plates and in locally thick sections of the bottom shell. These areas are typically the last to solidify during the forming process, which not only leads to the formation of shrinkage cavities and porosity, but also induces overall deformation of the casting due to localized thermal effects. In addition, residual stresses may develop at the connection interfaces, further compromising casting quality. Therefore, for such regions, an appropriately designed cooling system should be implemented to dissipate excess heat, thereby achieving simultaneous solidification across the entire casting and enhancing the uniformity and integrity of the final product.

initialization plays a crucial role in ensuring both the accuracy and efficiency of the model design. The width of each component represents the internal cross-sectional size of the cooling channel, the range of component width is 4–10 mm, and the range of component length is 15–40 mm. The orientation

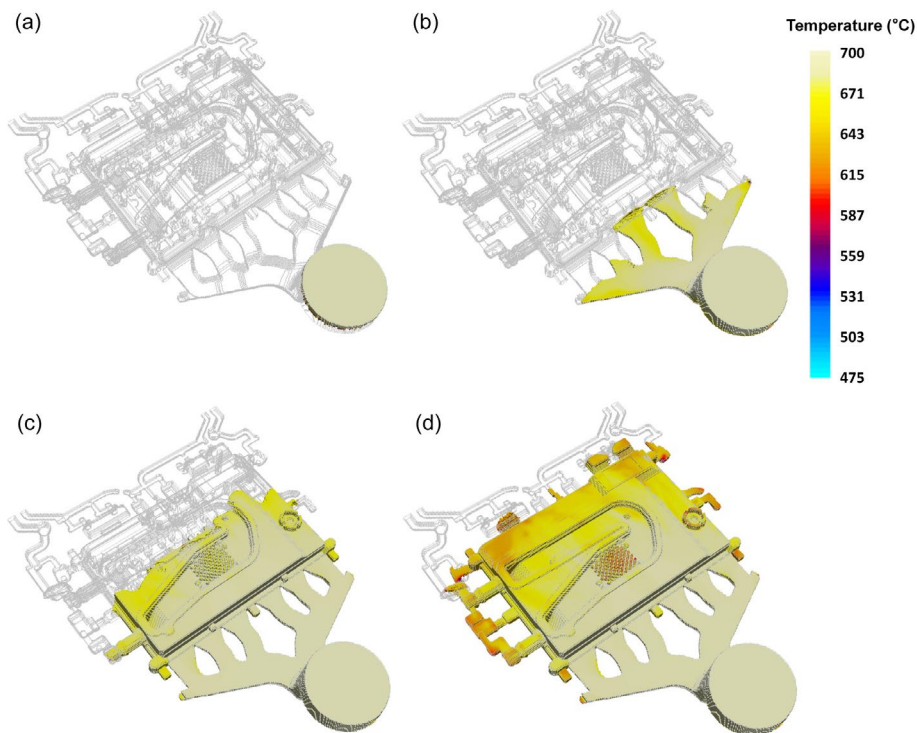


Fig. 3: Flow simulation results of the bottom shell casting: (a) $t=0.02$ s; (b) $t=0.10$ s; (c) $t=0.20$ s; (d) $t=0.35$ s

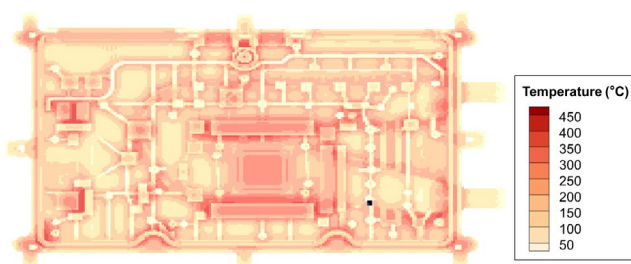


Fig. 4: 2D cross-section of temperature field of bottom shell casting

of each component is determined by the angle between its axial direction and the horizontal line. Four discrete angles are selected as the initial orientation options: 0° (180°), 45° (225°), 90° (270°), and 135° (315°). The number and spacing of components are equally important. Excessive density or an overly large number of components may result in redundant calculations and wasted computational resources, whereas overly sparse spacing or an insufficient number of components may lead to incomplete coverage of the design domain where cooling channels are required. Taking all these factors into consideration, the components are initialized. As shown in Fig. 5, a truss-like initialization scheme for the components is adopted. This is a typical initialization result of the cooling system.

4.2 Optimization results based on MMC method and PSO method

After completing the initialization of the components, the optimization of their spatial distribution was carried out based on the simulated temperature field and the PSO method described above. Two representative sets of model parameters

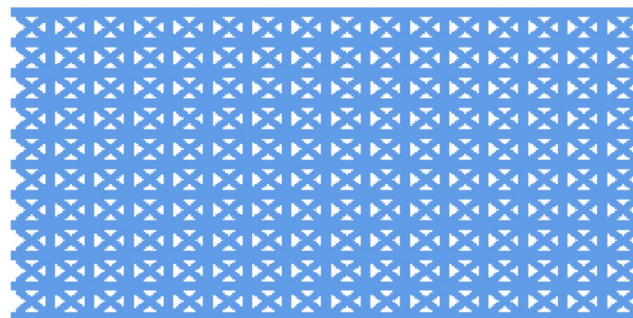


Fig. 5: A typical schematic diagram of component initialization scheme

were selected to compare the effects of different parameter configurations on the design outcomes. The specific values of the two parameter sets are listed in Table 4, and the corresponding optimization processes and final design results are illustrated in Fig. 6.

By analyzing the design processes and results under the two sets of model parameters (Fig. 6), it can be observed that all components follow the same optimization rule, gradually moving toward regions with higher temperatures in the thermal field. As the number of iterations increases, the number of components within the design space decreases. This reduction occurs because post-processing operations, such as merging and deletion, are applied after each iteration. Components located outside the design space are removed automatically. Between the two design schemes, the one with a larger number of components provides more comprehensive coverage of the overheated regions in the thermal field. However, its resulting configuration appears disordered and less consistent with practical cooling system design principles. Therefore, after

Table 4: Comparison of parameters for the two schemes

| Parameter | Number of initial components | Length (mm) | Width of the component (mm) | Angle | Step shift (mm) | Search radius in PSO method (mm) |
|------------|------------------------------|-------------|-----------------------------|--------------------|-----------------|----------------------------------|
| Scheme (A) | 1,200 | 20 | 4 | 0°, 45°, 90°, 135° | 2 | 20 |
| Scheme (B) | 800 | 30 | 6 | 0°, 90° | 4 | 30 |

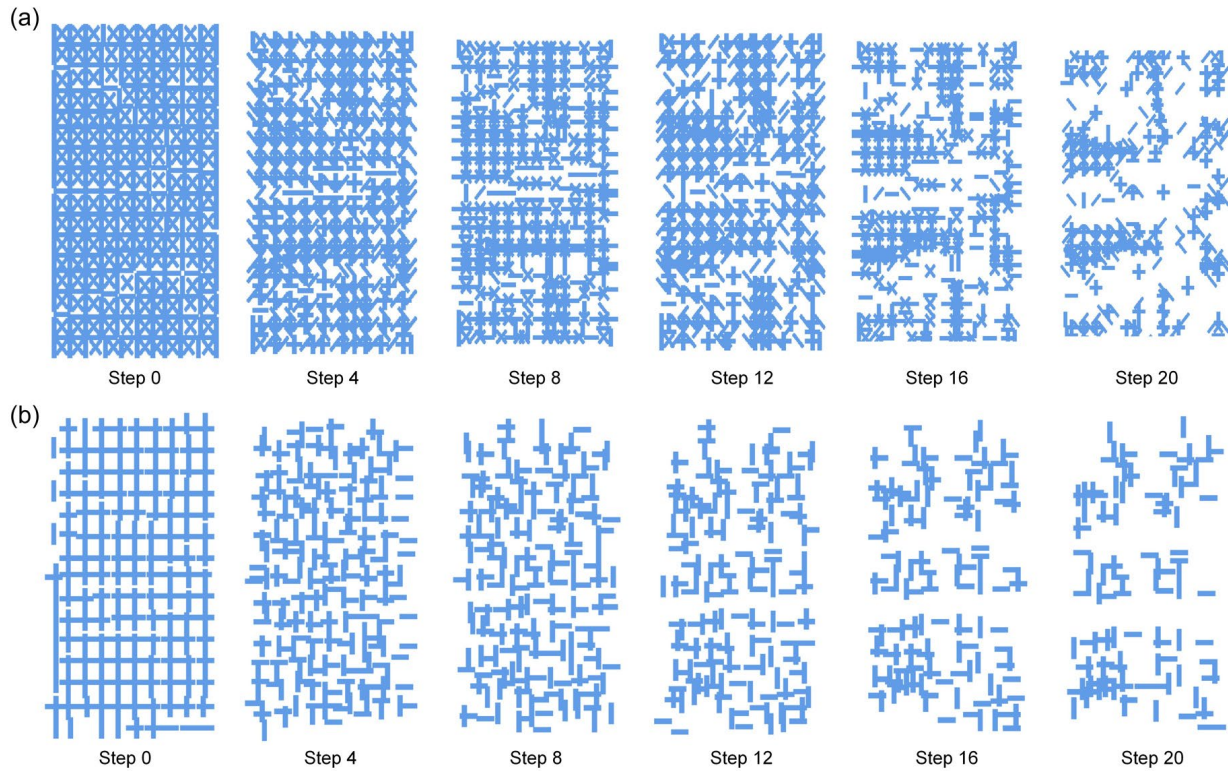


Fig. 6: Design process and results of the two schemes: (a) Scheme A; (b) Scheme B

a comprehensive comparison, the second design scheme is selected as the preferred solution.

Upon completion of the aforementioned component design, the resulting component layout cannot be directly utilized as cooling channels, since a cooling channel constitutes a unidirectional conduit with defined inlet and outlet points. Therefore, post-processing of the obtained component design is required, with the detailed procedure illustrated in Fig. 7. Firstly, the components are sorted based on the temperature field of the casting region they cover [Fig. 7(a)]. The sorting criterion stipulates that components covering regions with higher average temperatures are assigned higher priority. Subsequently, components at the end of the sorted sequence are eliminated [Fig. 7(b)]. As these correspond to casting regions with the lowest average temperatures, which require the least cooling. Next, since overlapping between different components may occur during the design process, one of the overlapping components is removed [Fig. 7(c)], following the same prioritization rule (i.e., the component with lower priority is deleted). Finally, the remaining valid components are interconnected [Fig. 7(d)] to ensure that the final design conforms to the physical requirements of a cooling channel system.

Following the post-processing operations described above, the final design of the cooling system was obtained. At this stage, a key adjustable parameter is the number of retained components, which has a significant impact on the design outcome. Figure 8 presents the final designs corresponding to different numbers of retained components, along with a comparison to a conventional cooling channel design. Comparing Figs. 8(a), (b), and (c), it can be seen that too few components (10 components) result in incomplete coverage of localized hot spots in the casting temperature field, whereas too many components (30 components) lead to manufacturability issues and produce a phenomenon similar to “overfitting” in machine learning. By balancing these considerations, the design with 20 retained components was selected. Figure 8(d) shows the conventional cooling channel design used as a reference. Comparing the selected design with the conventional one confirms the effectiveness of the cooling system layout generated by the present model.

4.3 Numerical validation of cooling system design

To validate the effectiveness and reliability of the proposed method, comparative simulations were performed under

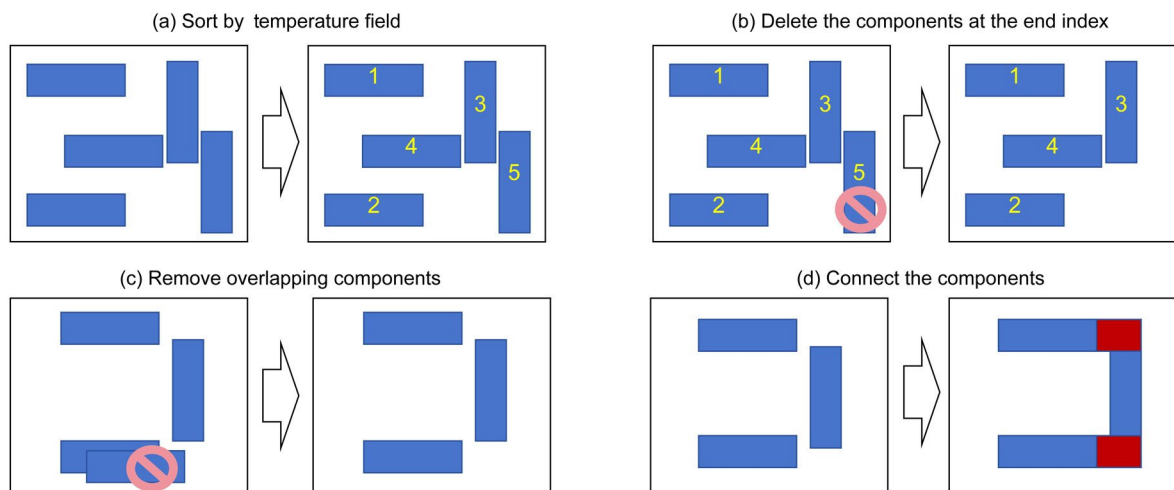


Fig. 7: Schematic diagram of component post-processing method (a-d)

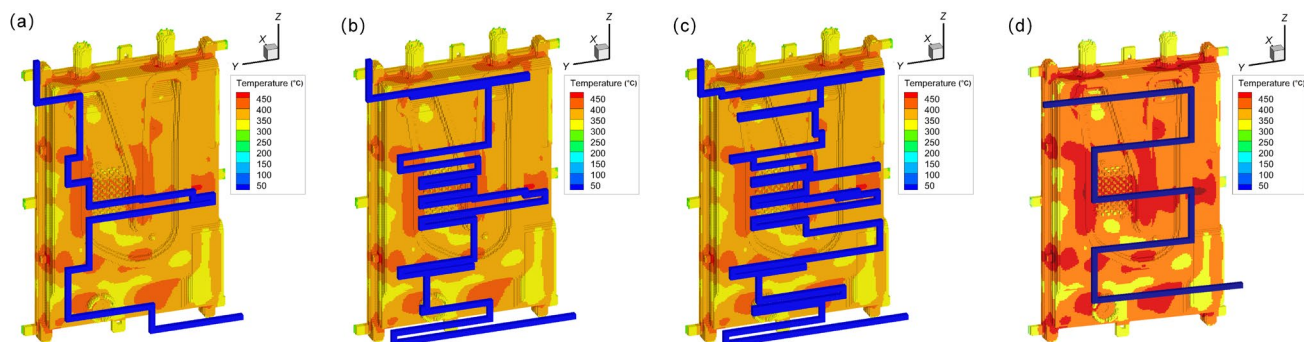


Fig. 8: Comparison of cooling system designs with different numbers of retained components and conventional cooling system: (a) 10 components; (b) 20 components; (c) 30 components; (d) conventional cooling system

identical process conditions for the filling and solidification processes of castings with and without the cooling system. Figure 9 shows a comparison of the temperature fields during different solidification stages. As observed, at various time points, the temperature distribution within the casting equipped with the cooling system exhibits better uniformity than that without cooling. This difference becomes increasingly pronounced after 150 s of solidification, as clearly demonstrated by the temperature fields highlighted within the red rectangles in the figure.

Figure 10 shows the comparison of the temperature field of the casting on a two-dimensional projection plane near the cooling system. It can be clearly seen that the overheating situation in the high-temperature areas has been significantly improved. Especially in the areas above 380 °C, it has almost completely disappeared. The thicker and larger the central part of the casting, the more obvious the temperature improvement effect.

The temperature field near the cooling channels was analyzed under three conditions: with a conventional cooling system, with the current cooling system, and without any cooling system. Figure 11(a) shows the standard deviation of the temperature field, which reflects the uniformity of cooling across the casting and is critical for preventing defects such as cold shuts and deformation. As shown in Fig. 11(a), after 30 s,

the standard deviation for castings with both the conventional and current cooling systems becomes significantly lower than that of the casting without a cooling system. Moreover, the current cooling system consistently exhibits a smaller standard deviation than the conventional system, indicating that it provides a more uniform cooling process during solidification. This difference continues to increase over time. Interestingly, after 90 s, the conventional system shows a higher standard deviation than the no-cooling case, likely due to its lower placement accuracy, which results in unnecessary cooling in regions where it is not required. In contrast, the current system maintains a lower standard deviation throughout the process, demonstrating its higher placement precision and effectiveness in enhancing cooling uniformity.

Figure 11(b) presents the average temperature of the castings under the three conditions. The average temperatures of the castings with the conventional and current cooling systems are similar at each time point and are consistently lower than those of the casting without a cooling system. This indicates that the improved cooling performance of the current system is not primarily due to an increase in the number of cooling channels, which would naturally reduce the average temperature, but rather results from the more precise placement of the channels. The close agreement in average temperatures between the conventional and current cooling

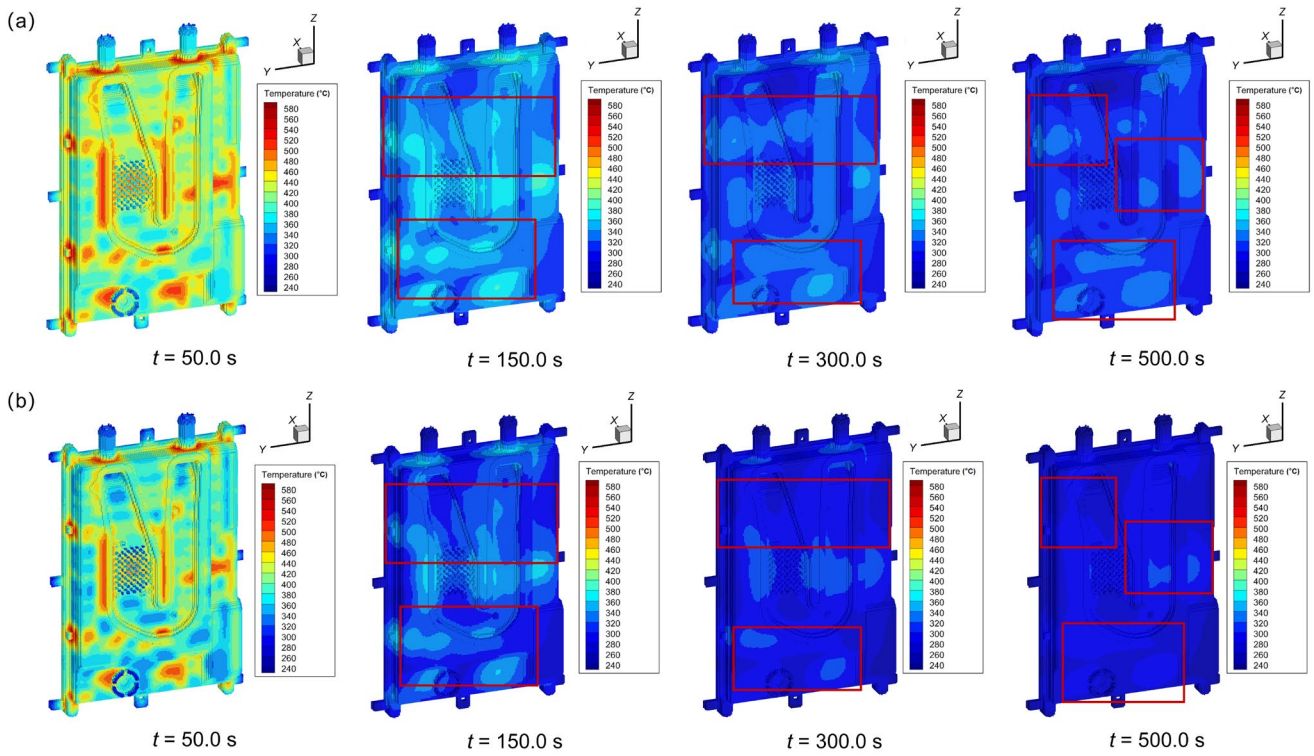


Fig. 9: Comparison of simulated casting temperature fields with versus without cooling system at different time instances: (a) without cooling system; (b) with cooling system

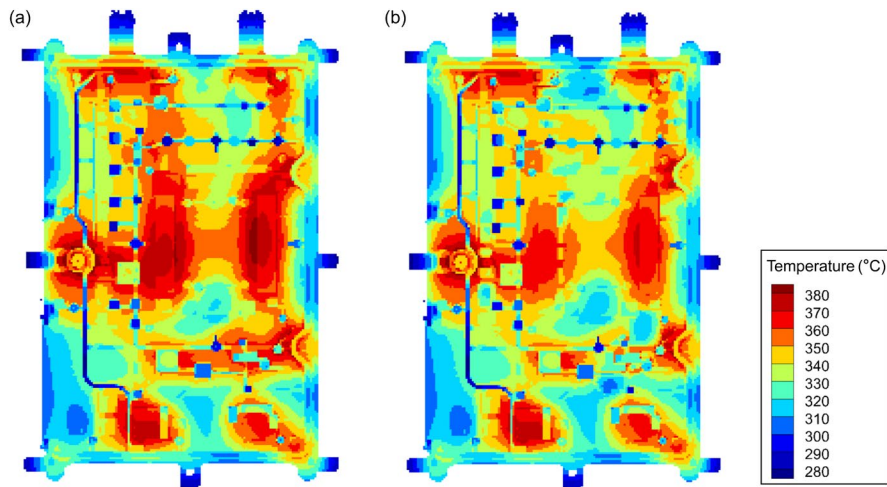


Fig. 10: Comparison of temperature field of casting on two-dimensional projection surface adjacent to cooling system: (a) without cooling system; (b) with current cooling system

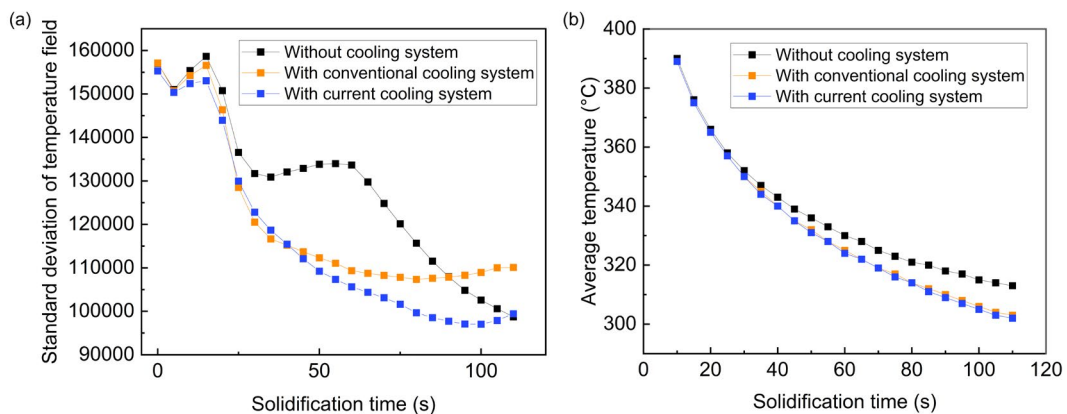


Fig. 11: Temperature field standard deviation for castings near the cooling channels in three different conditions (a) and comparison of average temperature (b)

systems demonstrates that the enhanced uniformity achieved by the current system arises from its optimized channel layout rather than simply increasing the cooling capacity. Together, these results validate the effectiveness of the current cooling system in simultaneously improving both the uniformity and efficiency of the solidification process.

5 Conclusions

This study proposes an automated design framework integrating the moving morphable components (MMC) topology optimization method with particle swarm optimization (PSO) to generate efficient and manufacturable cooling channel layouts. Based on the results of this study, the main conclusions are summarized as follows:

(1) The integrated MMC-PSO optimization framework successfully generates physically meaningful cooling channel layouts by driving morphable components to migrate toward high-temperature regions during the optimization process. Comparative analysis using castings with a conventional cooling system and without any cooling system as benchmark cases demonstrates that Scheme (B), initialized with 800 components and optimized parameters, yields a more practical and manufacturable cooling layout than the denser Scheme (A) with 1,200 components, while maintaining effective thermal coverage.

(2) The proposed post-processing strategy effectively ensures the manufacturability of the optimized designs. By incorporating temperature-based component sorting, removal of low-priority and overlapping components, and final channel interconnection, the optimized layouts are transformed into a continuous and physically realizable cooling system with unidirectional flow characteristics.

(3) Numerical simulations validate the thermal performance and robustness of the final optimized cooling system. Compared with both the conventional cooling system and the no-cooling case, the current design significantly alleviates overheating, with regions exceeding 380 °C almost completely eliminated, particularly in the thicker central regions of the casting. The optimized system consistently exhibits a lower temperature standard deviation after 30 s and maintains superior cooling uniformity throughout solidification, whereas the conventional system even shows a higher standard deviation than the no-cooling case after 90 s. Meanwhile, the average casting temperatures of the conventional and optimized systems remain comparable, confirming that the improved cooling performance arises primarily from more precise channel placement rather than increased cooling capacity. These results demonstrate the effectiveness of the proposed method in enhancing cooling uniformity and reducing defect risks such as cold shuts and deformation.

Acknowledgment

This work was financially supported by the National Natural Science Foundation of China (Grant No. 52435007).

Conflict of interest

Prof. Jian-xin Zhou is an EBM of *CHINA FOUNDRY*. He was not involved in the peer-review or handling of the manuscript. The authors have no other competing interests to disclose.

References

- [1] Niu Z C, Liu G Y, Li T, et al. Effect of high pressure die casting on the castability, defects and mechanical properties of aluminium alloys in extra-large thin-wall castings. *Journal of Materials Processing Technology*, 2022, 303: 117525.
- [2] Dong J, Jiang J F, Wang Y, et al. Research on numerical simulation and integrated die casting process of large complex thin-walled aluminum alloy automobile rear floor. *Results in Engineering*, 2025, 105399.
- [3] Zhan L, Sun Y M, Song Y, et al. Thin-walled and large-sized magnesium alloy die castings for passenger car cockpit: Application, materials, and manufacture. *China Foundry*, 2024, 21(5): 525–545.
- [4] Wang Q G, Wang A, and Coryell J. Ultra-large aluminum shape casting: Opportunities and challenges. *China Foundry*, 2024, 21(5): 397–408.
- [5] Li G L, Zhang J, Wang M Y, et al. Effect of mold and core preheating temperature on corrosion resistance of casting Al-12Si alloy U-shaped cooling channel. *China Foundry*, 2023, 20(3): 218–224.
- [6] Zhang Y X, Wang J S, Chen D X, et al. Effects of cooling rates on microporosity in DC casting Al-Li alloy. *China Foundry*, 2022, 19(2): 177–190.
- [7] Fiorentini F, Curcio P, Armentani E, et al. Study of two alternative cooling systems of a mold insert used in die casting process of light alloy components. *Procedia Structural Integrity*, 2019, 24: 569–582.
- [8] Chavan R, and Kulkarni P S. Die design and optimization of cooling channel position for cold chamber high pressure die casting machine. *IOP Conference Series: Materials Science and Engineering*, 2020, 810(1): 012017.
- [9] Pelaccia R, Negozi M, Donati L, et al. Efficiency of conformal cooling channels inserts for extrusion dies. *Procedia Manufacturing*, 2020, 47: 209–216.
- [10] Yavuz H, and Ertugrul O. Numerical analysis of the cooling system performance and effectiveness in aluminum low-pressure die casting. *International Journal of Metalcasting*, 2021, 15(1): 216–228.
- [11] Kurtulus K, Bolatturk A, Coskun A, et al. An experimental investigation of the cooling and heating performance of a gravity die casting mold with conformal cooling channels. *Applied Thermal Engineering*, 2021, 194: 117105.
- [12] Shu L, Zhang Z W, Ren Z H, et al. Design and simulation of conformal cooling for a die-casting mold insert. *Journal of Physics: Conference Series*, 2021, 1939(1): 012002.
- [13] Dhisale M, Vasavada J, and Tewari A. An approach to optimize cooling channel parameters of low pressure die casting process for reducing shrinkage porosity in aluminium alloy wheels. *Materials Today: Proceedings*, 2022, 62: 3189–3196.
- [14] Arunkumar K, Bakshi S, Phanikumar G, et al. Study of flow and heat transfer in high pressure die casting cooling channel. *Metallurgical and Materials Transactions: B*, 2023, 54(4): 1665–1674.
- [15] Zhang W S, Yuan J, Zhang J, et al. A new topology optimization approach based on moving morphable components (MMC) and the ersatz material model. *Structural and Multidisciplinary Optimization*, 2016, 53(6): 1243–1260.

- [16] Guo X, Zhang W S, Zhang J, et al. Explicit structural topology optimization based on moving morphable components (MMC) with curved skeletons. *Computer Methods in Applied Mechanics and Engineering*, 2016, 310: 711–748.
- [17] Zhang W S, Li D, Zhang J, et al. Minimum length scale control in structural topology optimization based on the moving morphable components (MMC) approach. *Computer Methods in Applied Mechanics and Engineering*, 2016, 311: 327–355.
- [18] Zhang W S, Li D, Yuan J, et al. A new three-dimensional topology optimization method based on moving morphable components (MMCs). *Computational Mechanics*, 2017, 59(4): 647–665.
- [19] Liu C, Zhu Y C, Sun Z, et al. An efficient moving morphable component (MMC)-based approach for multi-resolution topology optimization. *Structural and Multidisciplinary Optimization*, 2018, 58(6): 2455–2479.
- [20] Hou W B, Gai Y D, Zhu X F, et al. Explicit isogeometric topology optimization using moving morphable components. *Computer Methods in Applied Mechanics and Engineering*, 2017, 326: 694–712.
- [21] Takaloozadeh M, and Yoon G H. Implementation of topological derivative in the moving morphable components approach. *Finite Elements in Analysis and Design*, 2017, 134: 16–26.
- [22] Wang R X, Zhang X M, and Zhu B L. Imposing minimum length scale in moving morphable component (MMC)-based topology optimization using an effective connection status (ECS) control method. *Computer Methods in Applied Mechanics and Engineering*, 2019, 351: 667–693.
- [23] Sun Z, Song Z W, Song J F, et al. Structural optimization of fiber-reinforced material based on moving morphable components (MMCs). *Acta Mechanica Solida Sinica*, 2022, 35(4): 632–646.
- [24] Wang D S, Tan D P, and Liu L. Particle swarm optimization algorithm: An overview. *Soft Computing*, 2018, 22(2): 387–408.
- [25] Jain N K, Nangia U, and Jain J. A review of particle swarm optimization. *Journal of The Institution of Engineers (India): Series B*, 2018, 99(4): 407–411.